Er:YGG Planar Waveguides Grown by Pulsed Laser Deposition for LIDAR Applications

Jacob I. Mackenzie[a*], James A. Grant-Jacob[a], Stephen Beecher[a], Haris Riris[b], Anthony W. Yu[b], David P. Shepherd[a], and Robert W. Eason[a]
[a]Optoelectronics Research Centre, University of Southampton, SO17 1BJ, UK
[b] Laser & Electro-Optics Branch, NASA Goddard Space Flight Center, Greenbelt, MD 20771, U.S.A

ABSTRACT

Er:YGG planar waveguide amplifiers (PWAs) are promising candidates to meet the needs of greenhouse-gas differential-absorption LIDAR applications. We report pulsed–laser-deposition growth of this doped crystal and net-gain performance (internal gain ~2 dB/cm for 0.7-at.% Er-doping) in a 0.9-cm-long uncoated single-pass PWA. Rapid fabrication is also demonstrated with optimized parameters, where crystal growth rates approaching 20 microns/hour have been realized. We compare Er-doping concentrations ranging from 0.5 at.% - 4 at.%, and report on their spectroscopic properties. Furthermore, we show the ability to tailor the deposited crystal properties, controlling the waveguide and gain characteristics. Finally, we discuss the spectroscopy and potential performance of this relatively unstudied material for PWAs in the eye-safe regime.

Keywords: Planar waveguide amplifier; Erbium; Pulsed laser deposition; Crystal waveguides; LIDAR; Carbon dioxide and methane sensing

1. INTRODUCTION

Integrated Path Differential Absorption (IPDA) Lidar from earth-orbiting satellites provides a route to mapping, with unprecedented detail, various gaseous species in our atmosphere. For two key greenhouse gases, carbon dioxide (CO_2) and methane (CH_4), it is possible to exploit LIDAR in the 1.6-micron regime where there are suitable absorption features and excellent photodetectors. Planar waveguide amplifiers (PWAs) provide a route for achieving high gains in compact devices, through their ability to maintain strong population inversions over longer distances than is possible in equivalent bulk systems. Therefore, exploiting the Master Oscillator Power Amplifier (MOPA) configuration, direct amplification of low-powered single-frequency diode lasers up to the power levels required for LIDAR applications can be achieved. Er:YGG planar waveguides are promising PWA candidates, offering emission peaks aligned with key absorption bands of both gas species of interest. A crystalline host has potentially better power handling capabilities than glass equivalents and, due to the higher accessible gains, offer relatively short device lengths, which helps to raise the threshold for the onset of Stimulated Brillouin Scattering (SBS) that would degrade the spectral characteristics of the narrow-band seed. The PWA architecture has already been demonstrated in airborne campaign missions with Yb:YAG as the gain medium and proven that it is a viable candidate for such applications [1].

For this current work we are considering the garnet system containing yttrium and gallium, $Y_3Ga_5O_{12}$ (YGG), due to its favorable spectroscopic characteristics when doped with erbium [2-3]. YGG has an acceptable 2.2% lattice-constant mismatch with $Y_3Al_5O_{12}$ (YAG), which therefore provides a good substrate on which to grow these doped films. Furthermore, the difference in their respective refractive indices (1.91 for YGG and 1.82 forYAG) means that the resulting waveguide has a large numerical aperture of 0.58, well suited for high-power diode-laser pumping, either through proximity-coupling [4] or focused into the waveguide facets via end- or side-pumping configurations [5]. These features also lend themselves to large-mode-area “double-clad” or pump-guiding designs, which enable fundamental mode selection with the potential for high-power operation. Our preliminary studies have been focused on finding the optimum growth conditions for the Er:YGG crystal layers and assessing the potential emission and gain characteristics that will be needed for airborne LIDAR applications.

* J.I.Mackenzie@soton.ac.uk; phone +442380592693; www.orc.soton.ac.uk

2. METHODOLOGY

Pulsed Laser Deposition

As a mature physical vapor deposition process, pulsed laser deposition (PLD) is actually a relatively simple technology, and a detailed description of the setup we have used can be found in reference [6]. However, as a brief summary, PLD starts with a high-energy pulsed UV laser being focused onto a target in a controlled low-pressure background gas environment and the resulting plasma-plume propagates across the chamber and is deposited onto a heated substrate, as shown in Fig 1. Optimized growth of the desired crystal film nominally occurs when the substrate temperature is approximately half of the growing crystal's melting point. We use ceramic targets, which have lower ablation thresholds than single crystals and also cater for tailoring the composition of the target to control the grown crystal's stoichiometry [7]. With this approach, we have studied the growth of a wide range of oxides, including garnets [7] and sesquioxides [8], with the eventual aim of engineering the refractive-index profile and the spectroscopic properties on the sub-micron level.

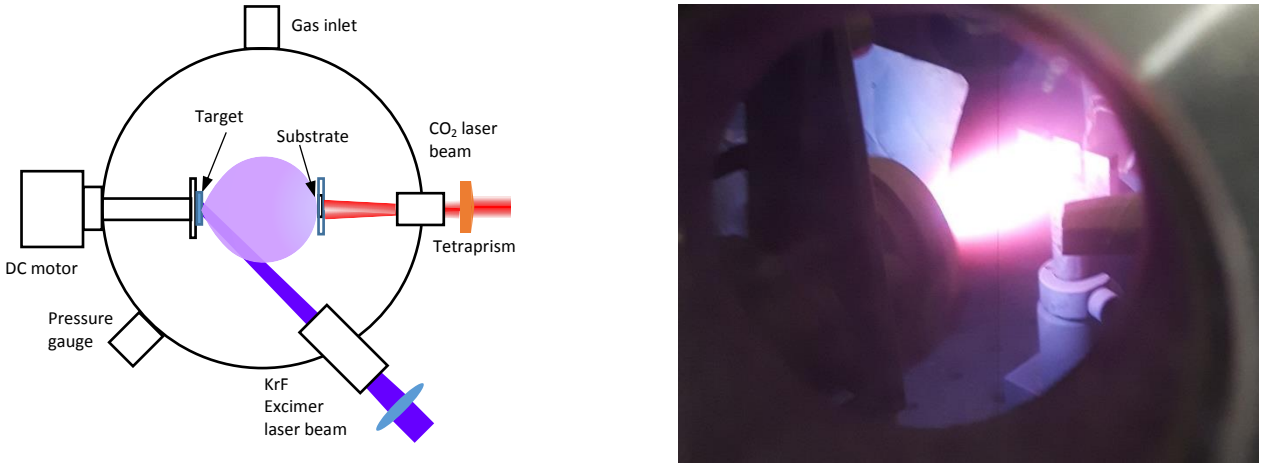

Fig 1. Schematic and photo of the PLD setup.

Two different KrF excimer lasers (Coherent - COMPexPRO) were utilized for growing the various garnet films, operating at repetition rates of 20 Hz or 100 Hz, the latter leading to ~20 μm/hour growth rates. At a wavelength of 248 nm, UV fluence levels of between 0.6 – 1.9 Jcm^{-2} were trialed, with the lower fluence levels typically providing smoother films but at a slower growth rate. The 1 mm-thick × $1cm^2$ substrate is heated with a homogenized CO_2 laser beam with incident powers ranging from ~10–25 W. There is no direct temperature measurement, as the repeatability based on incident power is sufficient. Several targets with various levels of gallium content were employed to assess the effect of compensating the loss of gallium that occurs between the ablation and deposition processes. To the best of our knowledge this is dependent upon two primary factors, namely scattering of the lighter element by heavier ones in the plasma plume and the volatility of gallium atoms on the heated substrate. In addition, a set of targets were made with different levels of erbium-doping, ranging from 0.5at.% - 4at.%. Films fabricated with these targets provided a set of waveguides with the potential for increasing gain per unit length and a route to analyze parasitic processes, such as energy-transfer upconversion (ETU).

Thin-film characterization

To determine that the grown crystalline layer is as intended, it is necessary to characterize several physical and optical properties of the film. The first key measurement is that of the lattice constant and crystallinity of the film, achieved using a Bruker D2 Phaser benchtop X-ray diffractometer, providing rapid assessment of the 2θ X-ray diffraction (XRD) spectra. Measurements of the composition of the respective films were made with a Zeiss EVO LS25 scanningelectron microscope (SEM) with an integrated Oxford Instruments INCAx-act X-ray detector for energy-dispersive X-ray analysis (EDX). Dark-field microscopy is undertaken with a Nikon LV100D optical microscope to assess the defect density of the films. While the morphology is measured with a white-light interferometer, Zemetrics – ZeScope, and/or KLA Tencor P-16 stylus profiler, which provide the values for the surface roughness and physical film thickness. The refractive index and waveguide properties of the crystal layers are measured with a Metricon (2010) m-line prism coupling system at a wavelength of 633 nm. This measurement also provides the film thickness and the number of supported modes in multimode waveguides.

Er:YGG characterization

To characterize the erbium spectroscopic properties we first measure the fluorescence from the top-face (perpendicular to the waveguide) of the Er:YGG film when excited with a suitable pump laser through the bottom-face of the double-side-polished substrate. The emission is collected with a multimode-fiber patch cable (0.22NA, 62 μm core fiber) held in close proximity to the excited film. An optical spectrum analyzer (OSA) (Ando AQ6317B) is used to record the emission spectra from the $^4I_{13/2}$ excited state. A very similar setup is used to determine the Er^{3+} lifetime, as shown in Fig. 2, with the same pump beam focusing arrangement but with free-space collection optics and pump filters imaging the fluorescence onto a transimpedance amplified InGaAs photodiode (Thorlabs PDA10CS-EC).

Waveguide propagation losses were determined using end-coupled lasers, initially a HeNe laser and then a tunable diode-laser in the telecoms band (Agilent 81689A), whereby the transmitted power through the polished waveguide end-facets is measured. Accounting for Fresnel reflection at the facets, the overlap efficiency of the incident beam and waveguide mode, and absorption by the erbium ions, an upper limit for propagation losses is calculated.

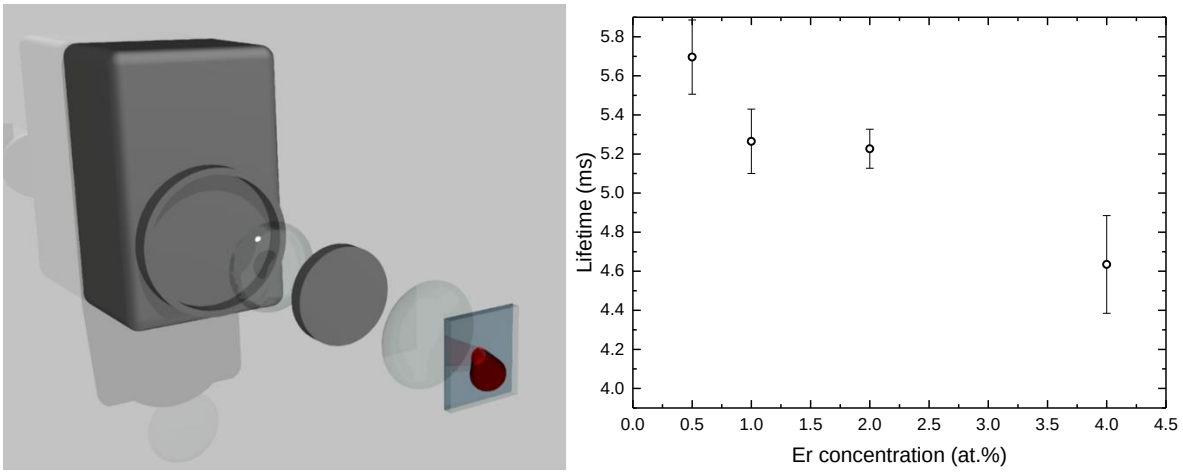

Fig 2. Illustration of the spectroscopic-measurements setup, and measured lifetimes for versus Er^{3+} concentration.

3. RESULTS

YGG layer growth

To assess the quality of the crystalline films we use XRD, as illustrated in Fig. 3, giving the lattice constant and crystallographic orientation. Fig. 3(a) shows the normalized 2θ spectra when varying the fluence on the target, in this case a 1at.% Er:YGG target, with 3% additional gallium in the form of Ga_2O_3 to offset its loss during the deposition process. For this composition there is a strong improvement in crystal quality as a function of increasing fluence, indicated by the sharpened peak and increasing 2θ position toward the expected value for the (222)-plane of pure YGG at 29.06°, marked by the dashed vertical lines in Fig. 3. It should be noted here that the diffractometer's copper X-ray source emits two wavelengths $\lambda_{\alpha 1}$ and $\lambda_{\alpha 2}$, which produces the dual-peak shape in the presented spectrum for what is a highly ordered single-crystal. It has been verified that by selecting just one X-ray wavelength the spectrum is indeed a single peak as expected.

A study of the effect of the relative gallium compensation in the target without any erbium doping was also investigated, the results being summarized in Fig. 3(b). It was found that with an increasing Ga-content the XRD 2θ peak position moved toward the theoretical value for YGG, with an optimum obtained with 9% additional gallium. From this we have now determined the optimum target composition to enable the fabrication of double-clad waveguide structures with a doped-YGG core, inner cladding layers of undoped YGG, and the outer cladding being the substrate and air interfaces.

Lastly, keeping the gallium compensation at 3at.%, we tested targets with different erbium concentration. As seen in Fig. 3(c), the addition of erbium into the targets/films leads to an increase in the XRD peak position, i.e. reduction of the lattice parameter. This is expected since $Er_3Ga_5O_{12}$ has a slightly smaller lattice constant than YGG, therefore the optimum 2θ peak position should be marginally higher than 29.06°, which will be achieved with increased Ga compensation.

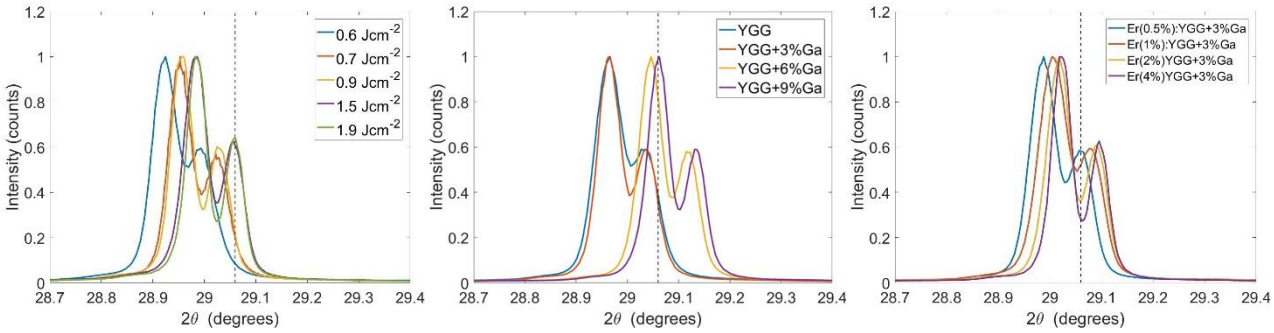

(a) (b) (c)

Fig 3 XRD 2θ spectra for YGG films (a) as a function of the UV laser fluence, (b) varying the gallium compensation in the target, and (c) as a function of the erbium concentration in the target.

As alluded to in the previous section, the proportion of Ga-atoms incorporated into the crystal lattice of the grown film was strongly linked to the temperature of the substrate. We observed an optimum in the relative gallium content in the film for a CO_2 laser power of around 9W, as determined via EDX and according to the stoichiometric value of 5 Ga-atoms per unit cell. These films were produced with a laser fluence of 1.3Jcm^{-2} operating at 100Hz in an O_2 background atmosphere at a pressure of 0.01 mbar and using the same target as for the results in Fig. 3(a). With less than 8W of incident CO_2 laser power the resulting film is amorphous, as the substrate is not hot enough to enable crystal growth, characterized by a drop in Ga-concentration and a strong decrease in refractive index. In line with the relative Ga-content in the grown films, there is a controllable refractive index dependence on substrate temperature, implying that the refractive index profile of the waveguide can be adjusted during the growth run by simply tuning the CO_2 laser power. The index changed from 1.935 at high temperature growth, to 1.938 near the optimum and decreasing down to 1.92 for amorphous growth.

Spectroscopic characterization

Upper-state lifetime measurements for the $^4I_{13/2}$ level were obtained for the four different doping levels trialed, as illustrated in Fig. 2, and found to be consistent with that of Stange *et al* [2]. It should be noted that the geometrically thin excitation region in our Er-doped film, leads to an effective "pinhole method" measurement [9] but without the need for an actual pinhole. As is typical for many rare-earth ions, with increasing erbium concentration there are quenching processes reducing the fluorescence lifetime [2].

Only two references were found with data on the spectroscopic characteristics for Er^{3+} impurities in the YGG host [2, 9], with which our measured fluorescence, Fig 5, compares extremely well. Emission cross section data was calculated using the Füchtbauer–Ladenburg equation, for two doping concentrations (4at.% and 0.7at.%) and with and without an additional 3% Ga compensation in the targets, respectively. We calculate the radiative quantum efficiency as the ratio of the measured lifetimes (4.65 ms and 4.8 ms, respectively) to the theoretical intrinsic lifetime of 7ms [10]. Furthermore, we use the reciprocity method to convert the emission-cross-section data into the absorption cross section, using the Stark energy levels in [10]. In both films we were able to discern features in the fluorescence around the 1550-nm region, Fig. 4(b) that could be associated with the Er^{3+} impurity substituting for Ga^{3+} in A-centers with C_{3i} symmetry [10]. However, with Ga-compensation, the strength of these lines was marginally weaker, indicating that there were less Er^{3+} substituting into these Ga^{3+} sites. Moreover, for the films without Ga-compensation the relative amplitude and bandwidths of the fluorescence peaks were slightly smaller and broader, compared to those with compensation.

Planar waveguide loss and gain measurements

For insertion-loss and gain measurements, light from the tunable diode laser and a 400 mW-1460 nm pump diode were combined using a wavelength division multiplexer (WDM). The output of the WDM was proximity coupled to a Corning HI1060 fiber, having a mode field diameter of 9.9 µm at 1550 nm, which in turn was proximity coupled to the planar waveguide entrance facet. Light from the waveguide was collected using two cylindrical lenses, f_x = 10 mm (unguided axis) and an f = 12 mm (guided axis), resulting in a near-symmetric and well-collimated output. Insertion-loss measurements (without pump) were taken at seven different wavelengths across the C- and L-bands and were used, along with the calculated spectroscopy for the Er:YGG (uncompensated film) in Fig. 4, to determine the background insertion loss (the insertion loss of the guide in the absence of absorption) and the dopant concentration in a manner similar to that reported by Parsonage et al. [8]. The results for the 9-µm-thick Er:YGG waveguide are displayed in Fig. 5, yielding a

background insertion loss of 1.95 dB and an Er ion concentration of 0.9×10^{20} ions.cm^{-3}, corresponding to a 0.7-at.% doping level. It should be noted that this doping level value only includes the N-center ions, which dominate the absorption and emission characteristics. For the background insertion-loss value we attribute 0.9 dB to Fresnel reflections from the two air-waveguide interfaces and 0.33 dB to coupling losses. Assuming the additional loss is entirely due to propagation loss, this places an upper limit on this value of 0.72 dB for the 9-mm guide or 0.80 dB/cm. Tests of the higher concentration waveguides are currently underway.

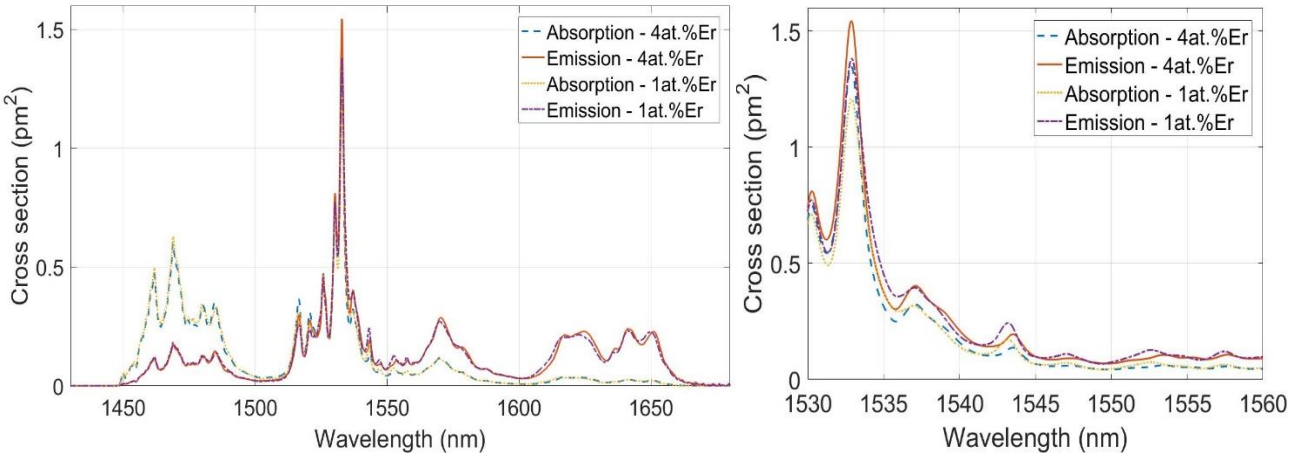

Fig. 4 (a) Absorption and emission cross sections for a 4at.% Er:YGG film (partially Ga-compensated) and the 1at.% Er:YGG with no Ga compensation. (b) Magnified view of the A-center peaks, matching reported energy levels in [10].

For the gain measurements a second pumping arrangement was also used. In that case the output of the HI1060 fiber was collimated and then coupled into the waveguide with two cylindrical lenses, firstly, to optimize the overlap of the guided mode and secondly to achieve confocal focusing, for the length of the waveguide, in the unguided direction. Gain measurements were performed for two seed wavelengths, 1533 nm and 1572 nm, in the symmetrical (fiber proximity coupled pumping) and confocal (cylindrical lenses pumping) configurations, as shown in Fig. 5(b). A photo of the symmetrically pumped waveguide is shown in the inset of Fig. 5(b), illustrating the signature green emission from the $S_{3/2}$ energy level of Er^{3+} populated by ETU processes.

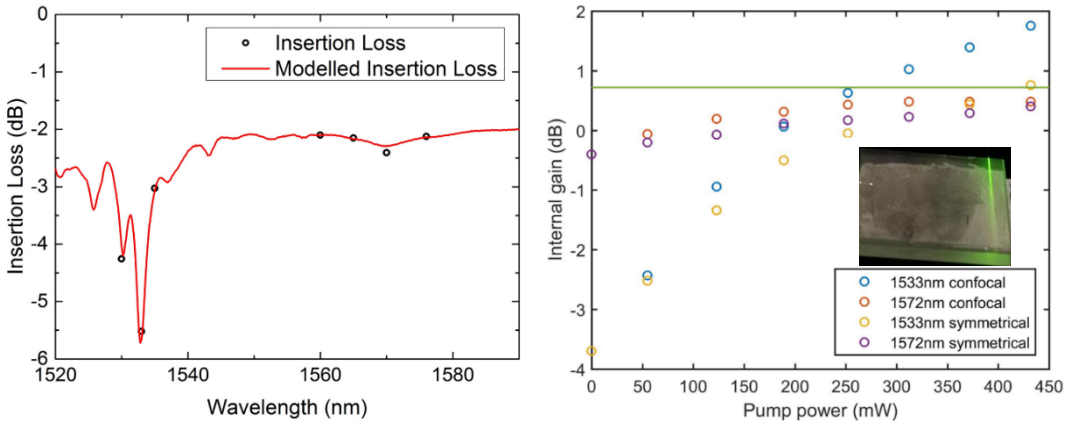

Fig. 5: Measured insertion loss and fit to absorption spectrum; internal net gain measurements (0.7at.% Er:YGG).

DISCUSSION

Waveguide losses

Whilst we have gain measurements as described above for the un-compensated Er:YGG waveguide, showing net gain over the propagation losses of the guide, the performance of our subsequent guides, which were 6-µm thick, was dominated by

scattering losses. These were the first trials with new targets and there is still scope to improve the results, nonetheless there are significantly more defect sites associated with the Ga-garnet materials (see Fig. 6 (a-b)), in comparison to previously reported Al-garnets (see Fig. 6 (c)), where losses are much lower [7].

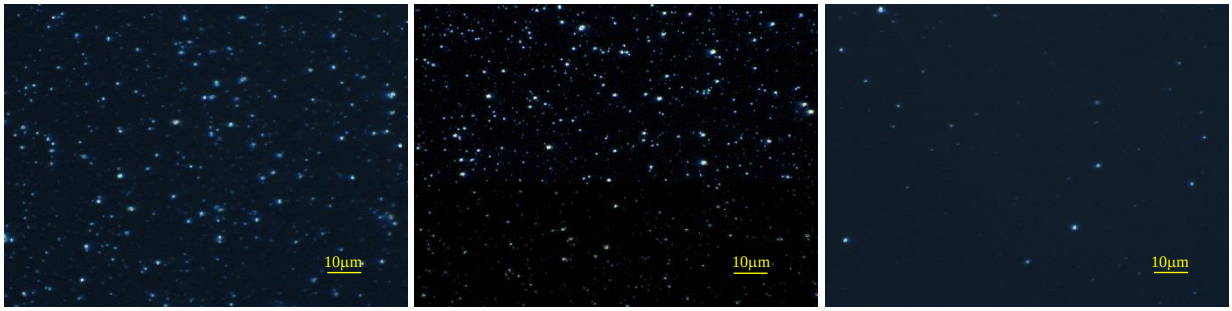

Fig. 6 Dark-field microscope images with 100x magnification of crystal waveguides fabricated from (a) 1at.% Er:YGG (b) 4at.%Er:YGG + 3% Ga, and (c) 7.5% Yb:YAG +3%Al, targets.

There are various areas to be addressed to tackle this particular issue, such as ensuring the target properties are conducive to particulate-free ablation or, in the more extreme case, exploiting velocity filters that block the slower travelling conglomerates propagating with the plasma plume.

Amplifier performance

As seen in Fig. 5, the amplified signals above the green horizontal line, representing the cumulative waveguide propagation losses, signifying internal net gain (assuming that the Fresnel reflections for each facet are ignored, as they can be nullified with anti-reflection coatings). For 1533 nm, we realized a 1.8 dB amplification (1dB internal net gain) with the confocal pumping configuration. For 1572 nm, a CO_2 absorption line, an internal gain of 0.5 dB was obtained (not quite overcoming the propagation loss). Therefore, to improve on this, three options are available; a) reduce the propagation losses (hence defects in the crystal film), b) increase the doping concentration to increase the gain per unit length (noting that quenching and ETU effects may well frustrate this goal), and c) consider waveguide designs that enable longer lengths of interaction, such as multi-pass schemes. Due to the similar emission cross-sections at 1572 nm and 1651 nm for this material, the observed gain at the former is representative of the expected gains achievable at the latter for similar pump and seed conditions.

4. CONCLUSIONS

We have, for the first time, fabricated and tested Er:YGG crystal films grown by pulsed laser deposition for planar waveguide amplifiers. Comparable spectroscopic parameters have been measured from our films to that obtained from Czochralski grown material.

Reaching this material quality has involved careful consideration of several growth parameters, including the lattice matching between the substrate and grown film and the transfer of material from target to substrate to achieve stoichiometric crystal growth. There are still challenges to address in terms of the number of defects in the grown films, which currently hamper efficient waveguide performance. Nonetheless, as we have demonstrated with Yb:YAG planar waveguides [7], there is a solution to obtain quality comparable to that obtained via traditional growth methods. From a spectroscopic point of view, a very slight improvement can still be made in the films to reach fluorescence properties indistinguishable from bulk material and where the Er^{3+} only occupies the yttrium sites in the lattice. With improvements in the film quality, Er:YGG waveguides are promising candidates for PWA in the spectral regions that cover both CO_2 and CH_4 absorption features.

REFERENCES

[1] Yu, A. W., Betin, A., Krainak, M. A., Hendry, D., Hendry, B., and Sotelo, C., "Highly efficient Yb:YAG Master Oscillator Power Amplifier Laser Transmitter for Future Space Flight Missions," OSA Technical Digest (CD). AW4A.26 (2012).

[2] Stange, H., Petermann, K., Huber, G., and Duczynski, E. W., “Continuous wave 1.6-micron laser action in Er-doped garnets at room-temperature,” Applied Physics B-Photophysics and Laser Chemistry, 49(3), 269-273 (1989).
[3] Kudryashov, I. , "Low Er-doped yttrium gallium garnet (YGG) as active media for solid-state lasers at 1651 nm," NASA Tech Briefs, 39(4), 50, (2015).
[4] Mackenzie, J. I., Li, C., Shepherd, D. P., Beach, R. J., and Mitchell, S. C., “Modeling of high-power continuous-wave Tm : YAG side-pumped double-clad waveguide lasers,” IEEE Journal of Quantum Electronics, 38(2), 222-230 (2002).
[5] Mackenzie, J. I., “Dielectric solid-state planar waveguide lasers: A review,” IEEE Journal of Selected Topics in Quantum Electronics, 13(3), 626-637 (2007).
[6] Grant-Jacob, J. A., Beecher, S. J., Parsonage, T. L., Hua, P., Mackenzie, J. I., Shepherd, D. P., and Eason, R. W., “An 11.5 W Yb:YAG planar waveguide laser fabricated via pulsed laser deposition,” Optical Materials Express, 6(1), 91-96 (2016).
[7] Beecher, S. J., Grant-Jacob, J. A., Hua, P., Prentice, J. J., Eason, R. W., Shepherd, D. P., and Mackenzie, J. I., “Ytterbium-doped-garnet crystal waveguide lasers grown by pulsed laser deposition,” Optical Materials Express, Submitted, (2017).
[8] Parsonage, T. L., Beecher, S. J., Choudhary, A., Grant-Jacob, J. A., Hua, P., Mackenzie, J. I., Shepherd, D. P., and Eason, R. W., “Pulsed laser deposited diode-pumped 7.4 W Yb:Lu_2O_3 planar waveguide laser,” Optics Express, 23(25), 31691-31697 (2015).
[9] Kuhn, H., Fredrich-Thornton, S. T., Kränkel, C., Peters, R., and Petermann, K., “Model for the calculation of radiation trapping and description of the pinhole method,” Optics Letters, 32(13), 1908-1910 (2007).
[10] Ashurov, M. K., Voronko, Y. K., Osiko, V. V., Sobol, A. A., and Timoshechkin, M. I., “Spectroscopic study of stoichiometry deviation in crystals with garnet structure,” Physica Status Solidi A-Applied Research, 42(1), 101-110 (1977).